

Supplemental Data for Presence of substrate aids lateral gate separation in LptD

Karl P. Lundquist and James C. Gumbart*

School of Physics, Georgia Institute of Technology, Atlanta, GA 30313

* To whom correspondence should be addressed; Email: gumbart@physics.gatech.edu;

Phone: 404-385-0797

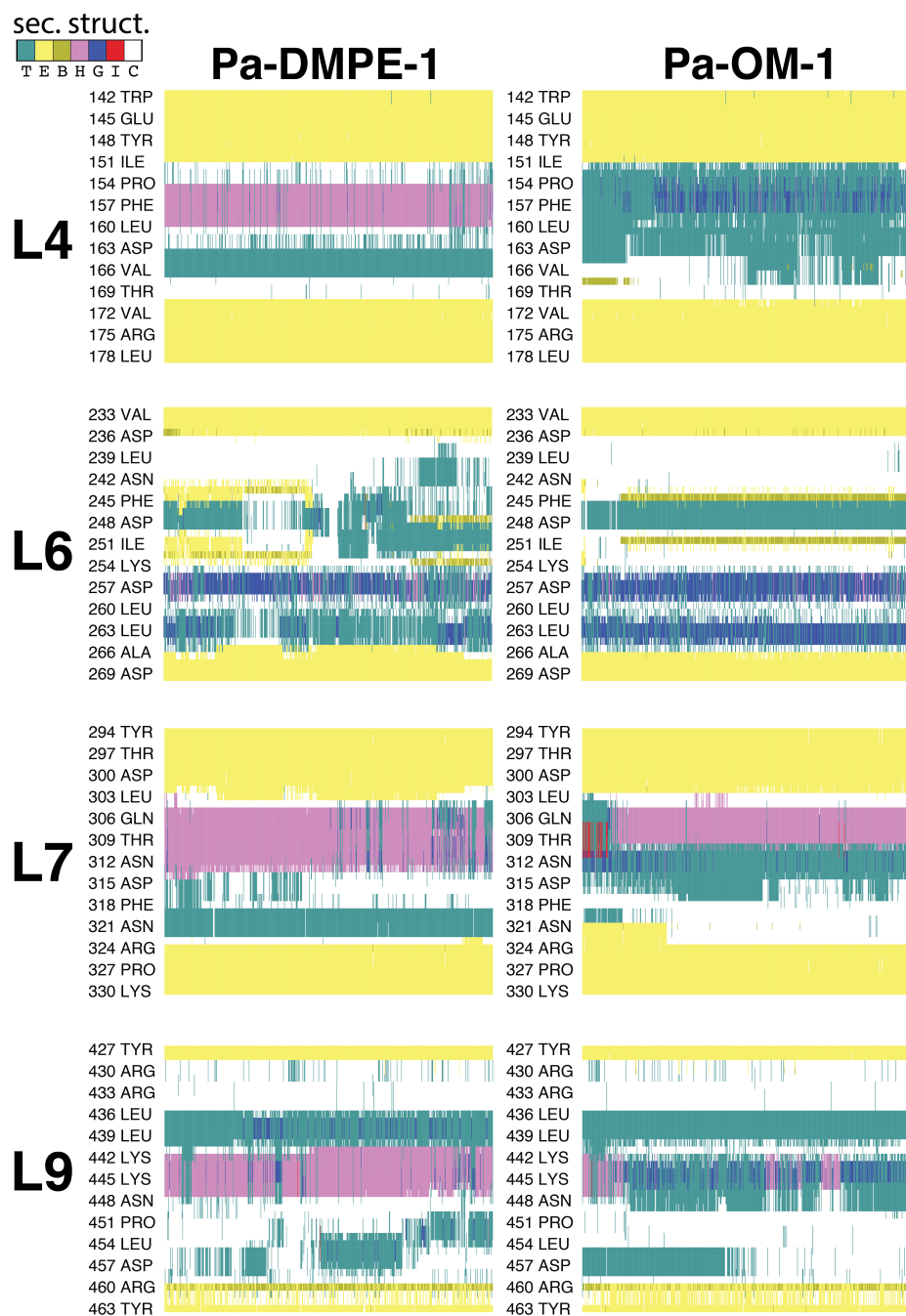


Figure S1: Secondary structure for extracellular loops as shown by the VMD timeline plugin. The traces shown are for the first 1.5 μ s of Pa-DMPE-1 and Pa-OM-1 for DMPE and OM respectively. Secondary structure codes are T (turn, cyan), E (extended β conformation, yellow), B (isolated bridge, gold), H (α -helix, pink), G (3_{10} -helix, blue), I (π -helix, red), and C (random coil, white).

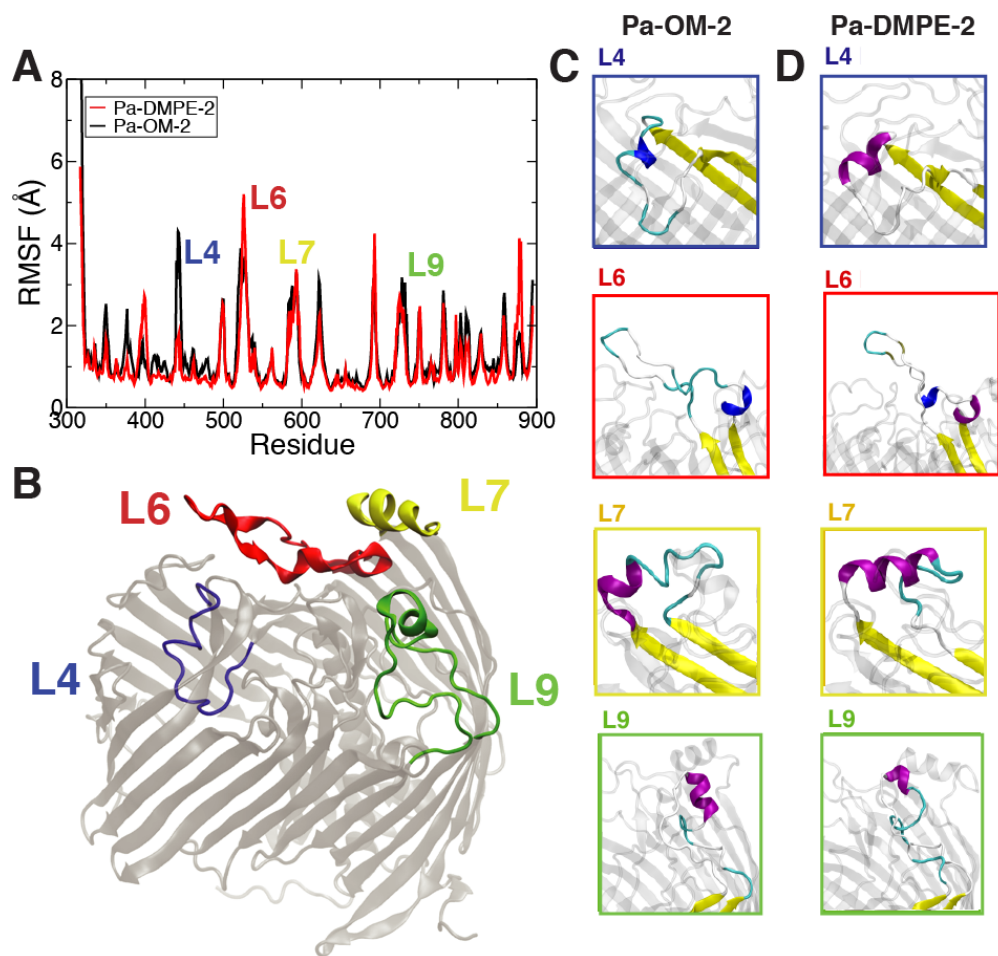


Figure S2: PaLptDE structure and dynamics for the second runs in DMPE and in OM. (A) Root-mean-square fluctuation (RMSF). (B) Location of key loops with respect to the overall structure. (C, D) Secondary structure comparison for the same loops as in Fig. 3 in the main text, namely L4 (blue), L6 (red), L7 (yellow) and L9 (green).

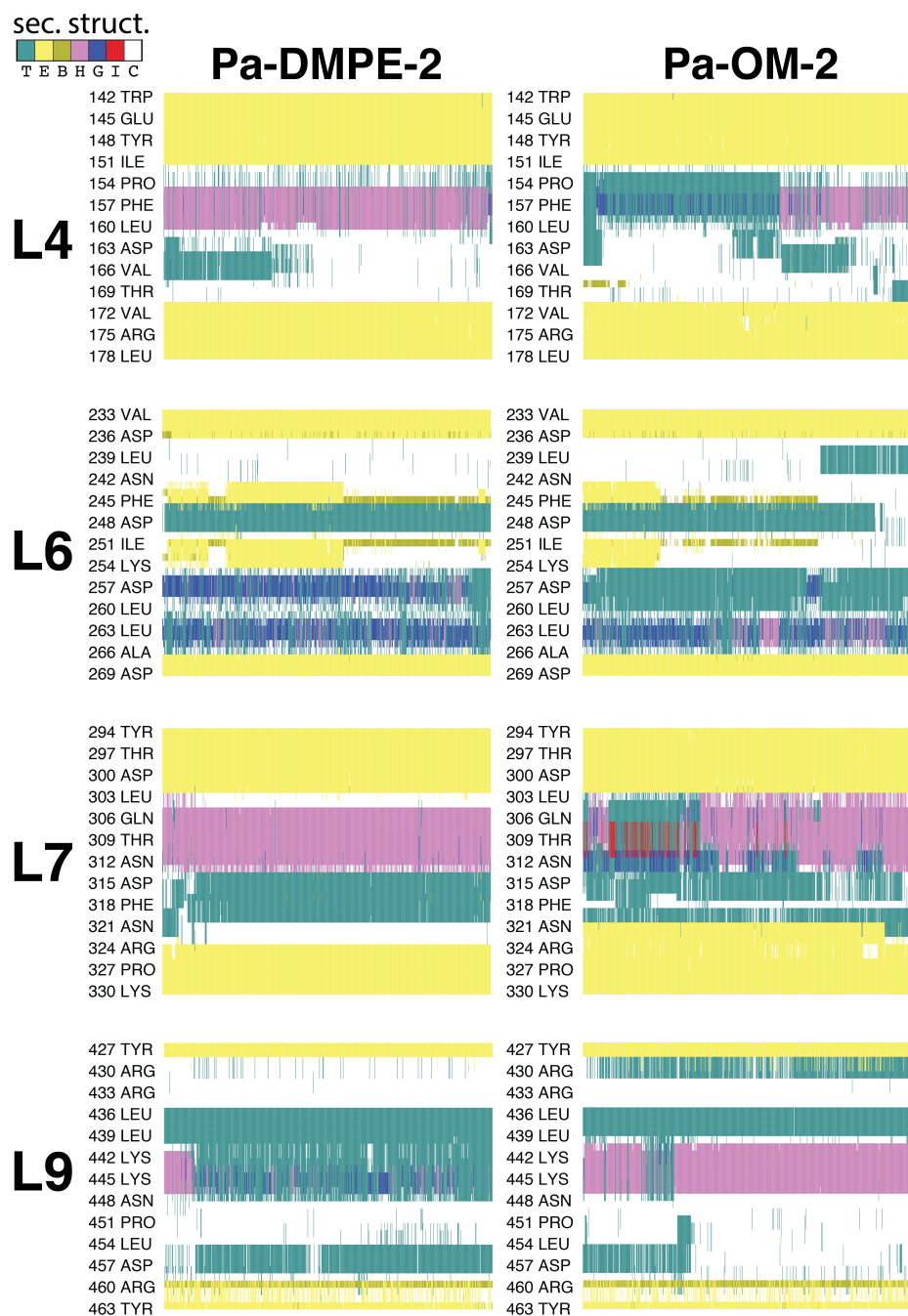


Figure S3: Secondary structure for extracellular loops as shown by the VMD timeline plugin. The traces shown are for the first 1.5 μ s of Pa-DMPE-2 and Pa-OM-2 for DMPE and OM respectively. Secondary structure codes are T (turn, cyan), E (extended β conformation, yellow), B (isolated bridge, gold), H (α -helix, pink), G (3_{10} -helix, blue), I (π -helix, red), and C (random coil, white).

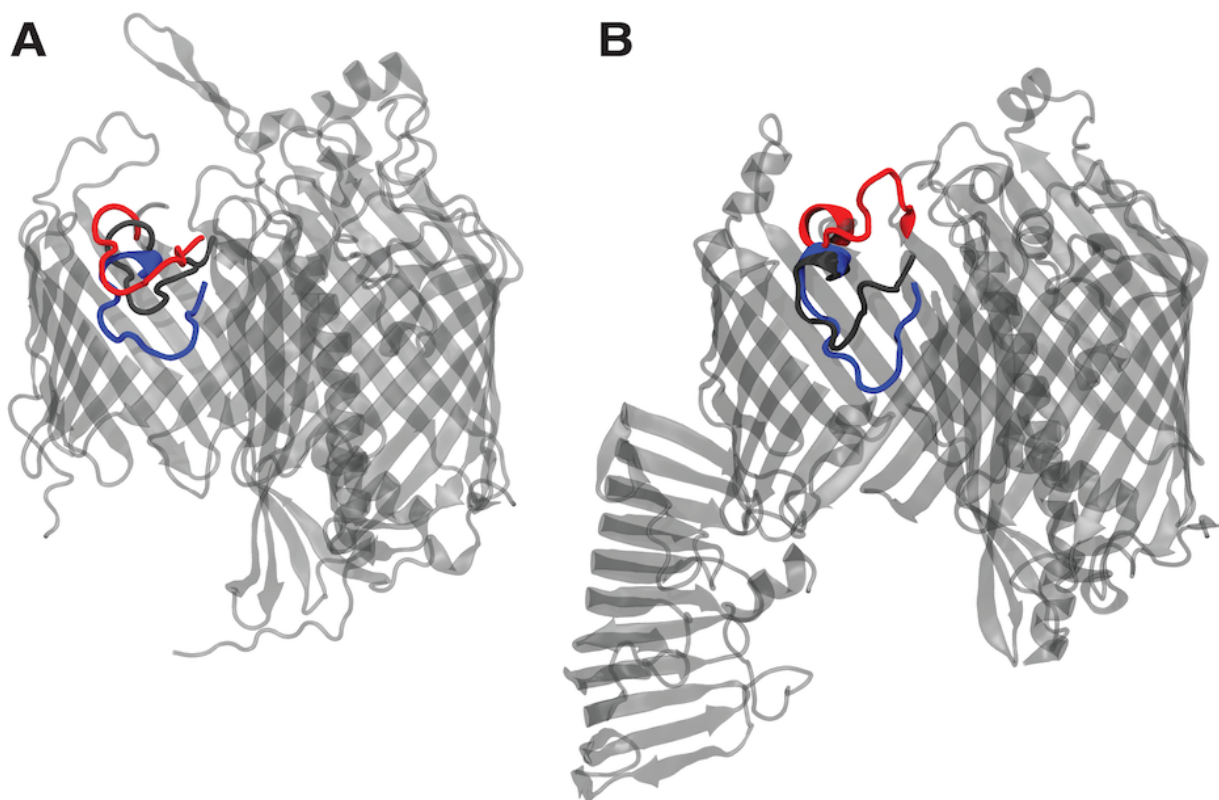


Figure S4: L4 position for the minimum (blue), maximum (red), and crystal structure (dark gray) from (A) PaLptDE simulations and (B) SfLptDE simulations. Crystal structures (PDBs: 5IVA and 4Q35, respectively) are shown as gray transparent ribbons for reference.

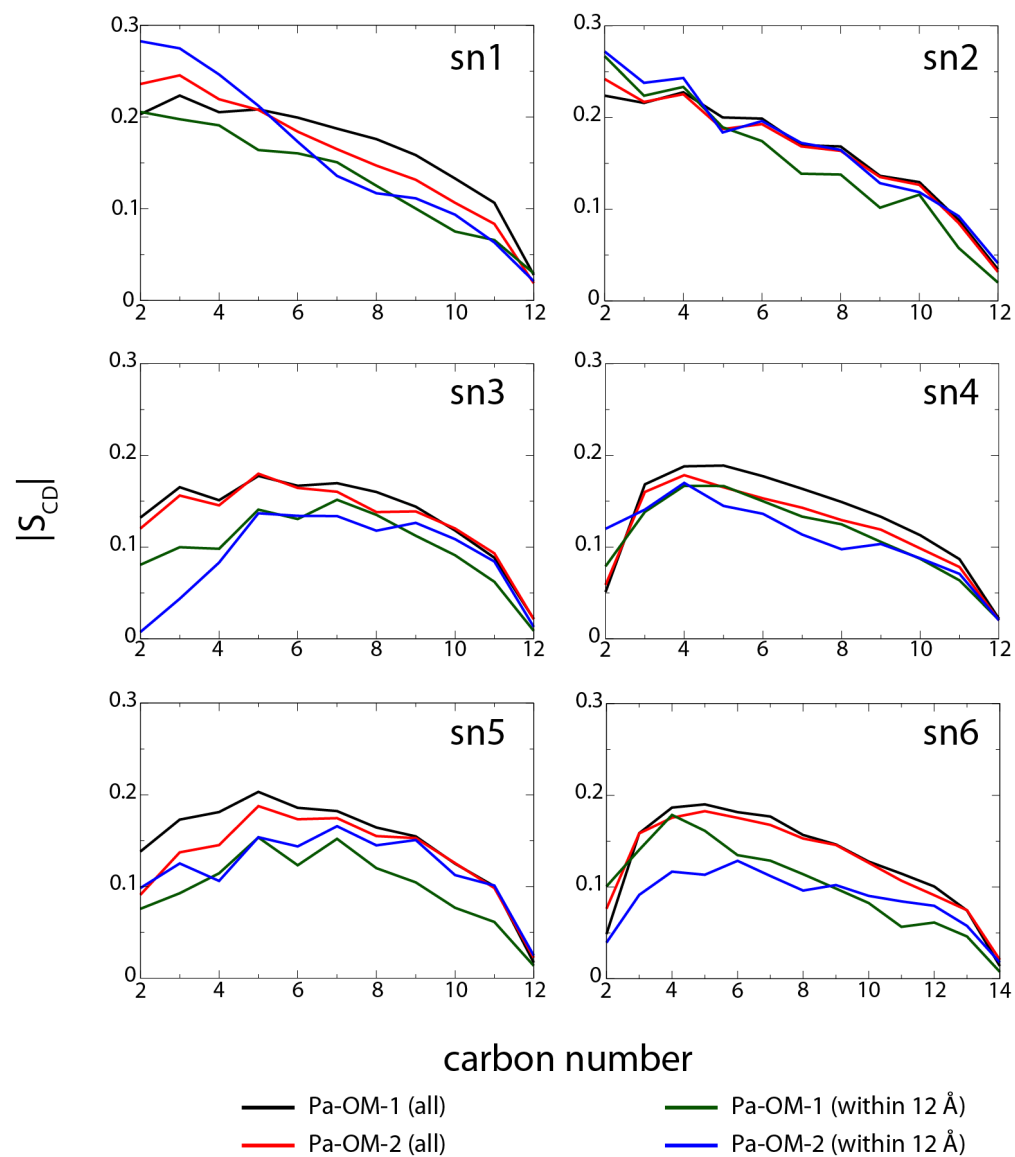


Figure S5: Deuterium order parameters of LPS acyl tails. In each plot, the black and red curves are for the given tails averaged over the entire membrane for the Pa-OM-1 (black) and Pa-OM-2 (red) simulations. The green and blue curves are for the given tails averaged over only those eight LPS molecules within 12 Å of LptD's lateral seam.

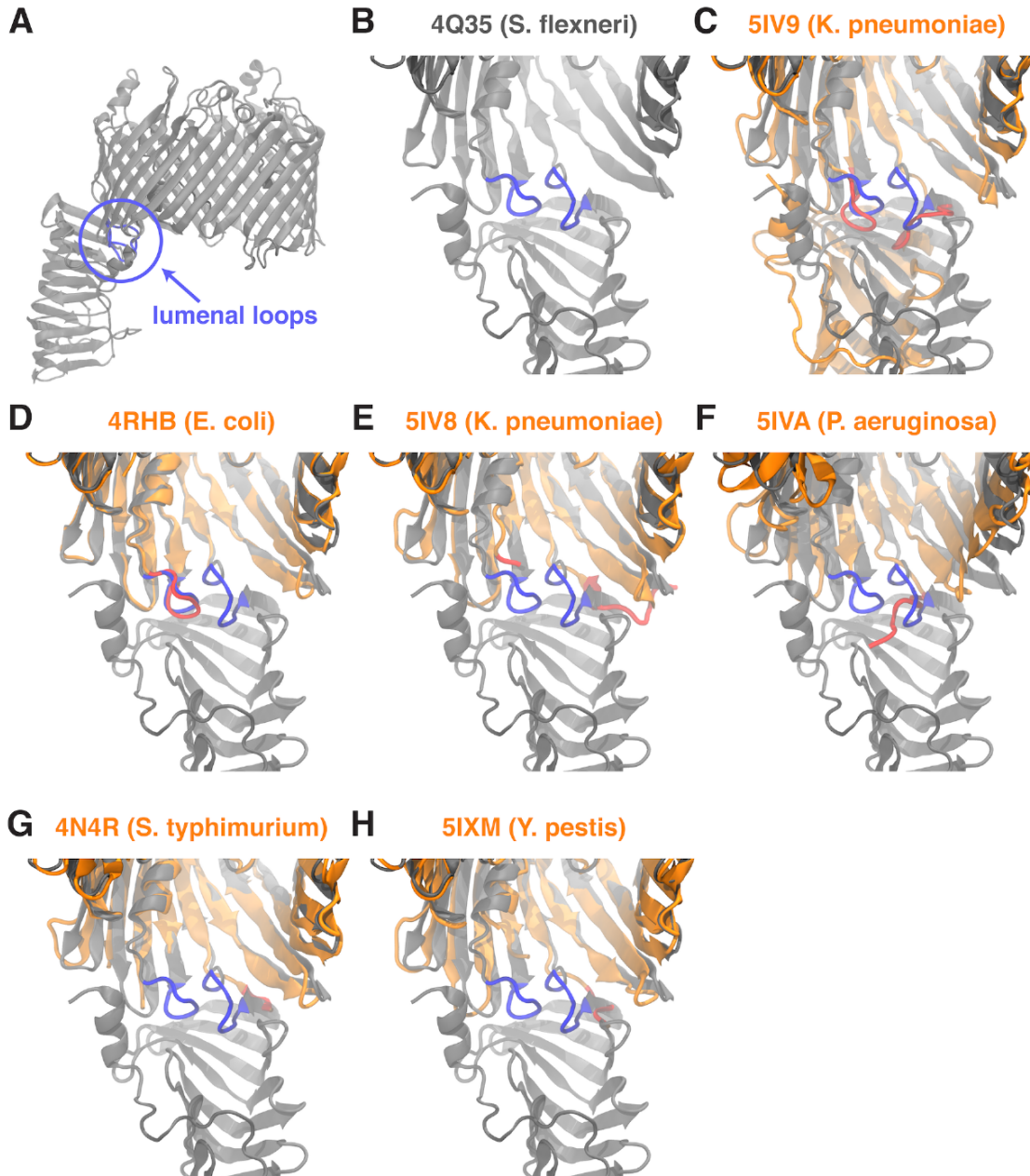


Figure S6: Positions of the luminal loops. (A) side view of LptD from *S. flexneri* with the luminal loops shown in blue. (B) View of luminal loops in SfLptD from the periplasmic side. This view of SfLptD is repeated in each of the following panels for reference. Both loops are in the closed position in PDBs 4Q35 (B) and 5IV9 (C). Loop 1 is closed and loop 2 is disordered in PDB 4RHB (D). Loop 1 is disordered and loop 2 is open in PDB 5IV8 (E). Loop 1 is disordered and loop 2 is closed in PDB 5IVA (F). Loop 1 is disordered and loop 2 is open in PDBs 4N4R (G) and 5IXM (H).

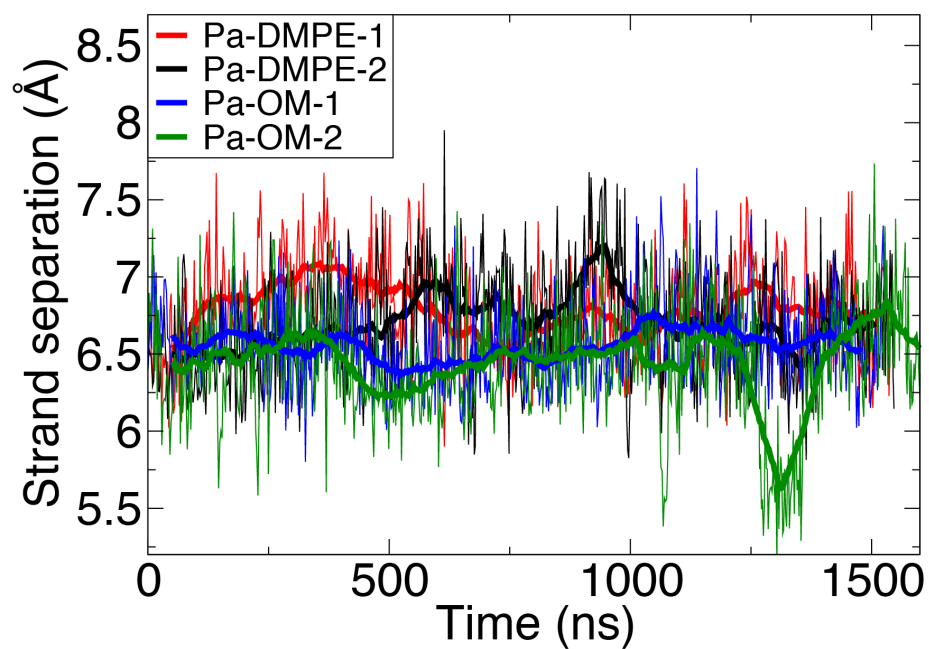


Figure S7: Separation of $\beta 1$ and $\beta 26$ strands vs. time for PaLptD. $\beta 1$ was defined as the C_{α} atoms of residues 325 to 334 and $\beta 26$ as those of residues 886 to 895. A 100-ns moving average has been added on top of the raw data. OM systems exhibit a slightly lower average separation value. Average values are 1.0 to 1.5 Å higher than in the Sf-apo system (see Fig. 6 in the main text), likely due to the absence of the N-terminal domain.

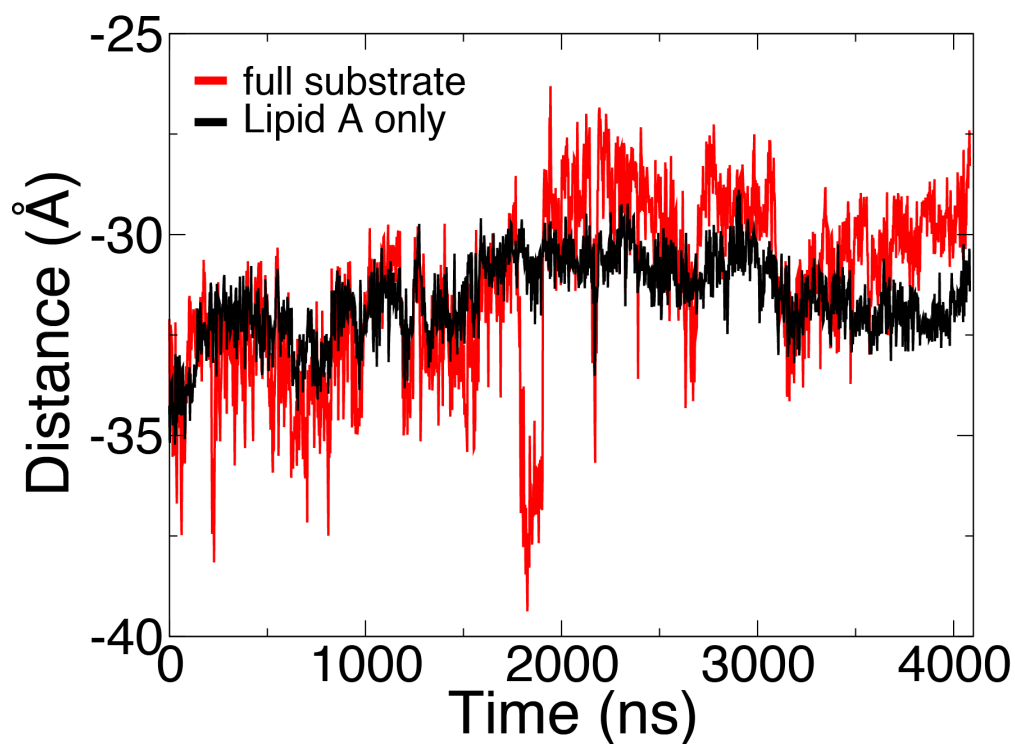


Figure S8: Center-of-mass distance from the center of the membrane for the substrate LPS molecule (red) and the Lipid A portion of the substrate (black) in Sf-LPS. The range of motion for Lipid A (between -35 and -30 Å) is smaller than that of the entire substrate (between -39 and -26 Å) due to being constrained within the interior of the LptD N-terminal domain. The large fluctuations in the position of the substrate core oligosaccharide result in a greater range of motion when measuring the position of the entire LPS substrate.

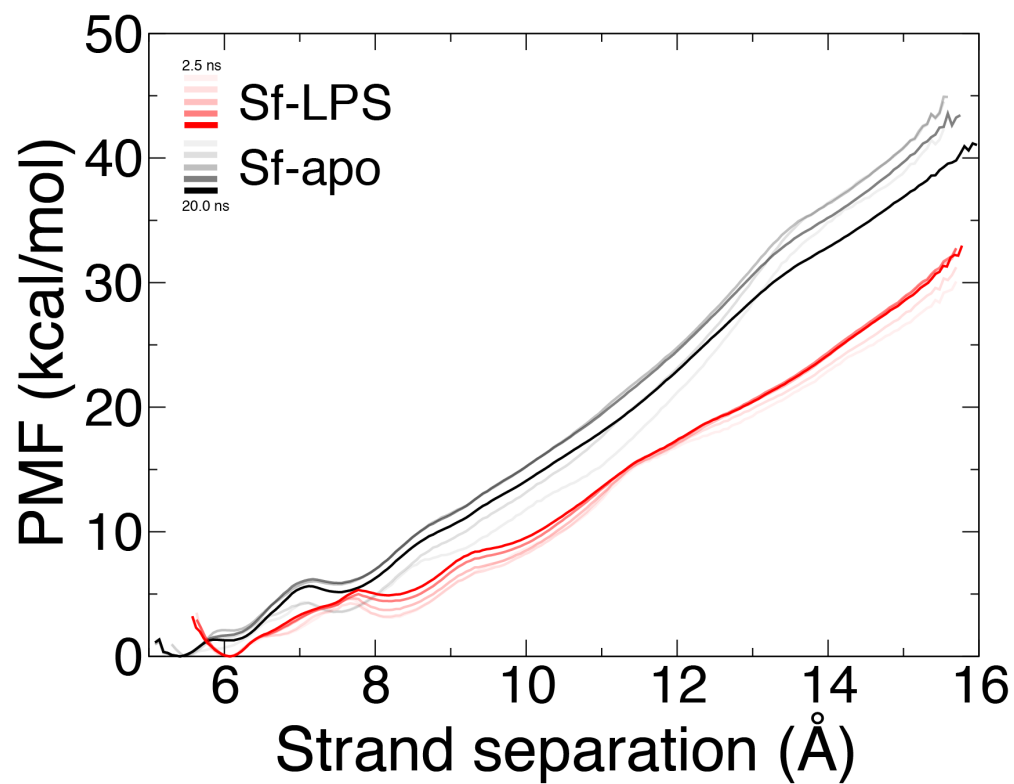


Figure S9: Convergence of PMFs for Sf-LPS and Sf-apo. PMFs are shown for 2.5, 5.0, 10.0, 15.0, and 20.0 ns/window in order of opacity with 2.5 ns/window shown at the lowest opacity, and 20.0 ns/window shown at the highest.

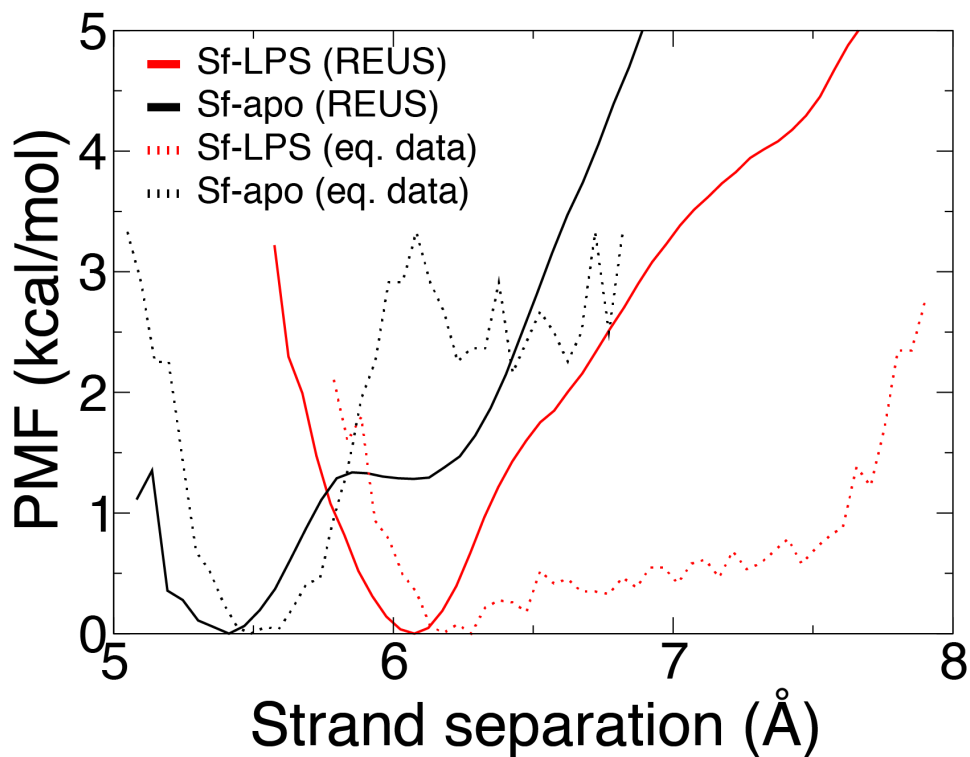


Figure S10: PMFs generated from equilibrium simulation data (dotted lines) plotted alongside the respective PMFs generated using REUS (solid lines). REUS data is also shown in Fig. 6B of the main text. These equilibrium-based (eq.) PMFs demonstrate a similar position of minimum energy when compared to their respective REUS PMFs. The eq. PMF for Sf-LPS is significantly lower than its respective REUS PMF for strand separation values above the minimum energy position. This likely indicates that one or more lower energy states for Sf-LPS were not properly sampled within the simulation time of the REUS calculation. However, when comparing the two eq. PMFs, the main results still hold true with respect to the shifted minimum position upon substrate binding and lowering of the energetic landscape.